

Article

Ceramic Papers as Structured Catalysts: Preparation and Application for Particulate Removal

Sabrina A. Leonardi, Eduardo E. Miró and Viviana G. Milt *

Instituto de Investigaciones en Catálisis y Petroquímica, INCAPE, Facultad de Ingeniería Química, Universidad Nacional del Litoral, CONICET, Santiago del Estero 2829, Santa Fe 3000, Argentina

* Correspondence: vmilt@fiq.unl.edu.ar

Abstract: Fibers represent a type of structure of great interest in catalysis since they combine high area to volume ratio and can be fabricated from many types of materials, such as ceramic oxides, polymers, and alloys. They can be used in isolated form or structured, as in the case of the ceramic papers synthesized in this work, following a modified papermaking technique. The addition of cationic and anionic polyelectrolytes improved the retention of ceramic fibers during the ceramic paper formation stage by adsorption processes, through the formation of floccules. In the complex aqueous system containing charged macromolecules, the amounts of polyelectrolytes to be added were determined by titrations. To enhance mechanical properties of ceramic papers, different classes of nanoparticle suspensions can be used as binders. As a novel alternative, we have used different borate-type compounds. Among them, we selected natural ulexite, which was purified and used as a binder of ceramic fibers. In order to improve mechanical resistance and flexibility, measured from tensile indexes and elastic module, the amounts of $\text{NaCaB}_5\text{O}_6(\text{OH})_6 \cdot 5\text{H}_2\text{O}$ and the calcination temperature were varied. In this contribution, to take advantage of the unique characteristics of the ulexite-containing ceramic papers, they were impregnated with Co,Ce and Co,Ba,K and tested for diesel soot combustion.

Keywords: ceramic papers; ulexite binder; polyelectrolyte titration; Co,Ce and Co,Ba,K catalysts; carbonaceous particles



Citation: Leonardi, S.A.; Miró, E.E.; Milt, V.G. Ceramic Papers as Structured Catalysts: Preparation and Application for Particulate Removal. *Catalysts* **2022**, *12*, 1153. <https://doi.org/10.3390/catal12101153>

Academic Editors: Marcela Martínez Tejada and Miguel Ángel Centeno

Received: 1 September 2022

Accepted: 28 September 2022

Published: 1 October 2022

Publisher's Note: MDPI stays neutral with regard to jurisdictional claims in published maps and institutional affiliations.



Copyright: © 2022 by the authors. Licensee MDPI, Basel, Switzerland. This article is an open access article distributed under the terms and conditions of the Creative Commons Attribution (CC BY) license (<https://creativecommons.org/licenses/by/4.0/>).

1. Introduction

Carbonaceous particles are emitted from different sources where combustion processes take place. Among these processes, different types of industries, power plants, and means of transport can be considered as soot generators. Domestic uses should also be included as sources of soot particulate emissions, with cooking and heating being good examples [1]. In general, soot particles are carriers of harmful organic compounds, and exposure to them can cause various diseases and are, therefore, of public concern [2]. Diesel engines are considered to be one of the main sources of soot, however, Otto engines also emit these particles, albeit to a lesser extent. It is now accepted that it is not only the mass emitted by vehicles that is important, but also the size of the particles, since the smaller the size, the greater the penetration into the lungs [3]. Therefore, care must be taken with both the mass and the number of particles emitted.

It is generally accepted that filtration is the best way to remove particulates, but filters should be cleaned periodically. In the case of carbonaceous particles, combustion is the most effective form of regeneration. Since high temperatures are necessary for thermal combustion, the presence of a combustion catalyst could help in the regeneration process. In the case of the use of filters to remove soot from diesel engines, they are called diesel particulate filters (DPFs) [4,5].

Typically DPFs are made of ceramic materials, such as cordierite and silicon carbide. In our research group, we have proposed lower cost and high efficiency alternatives, consisting

of catalytic metal mesh cartridges [6], catalytic ceramic papers [7] and combinations of them, which were successfully evaluated both in laboratory and in a bench diesel engine.

In the case of catalytic papers, they are composed of a mat of ceramic fibers formed with the aid of a binder material. An easy method to synthesize these ceramic papers is through a modification of the conventional papermaking technique. The role played by the binder is fundamental, since it is responsible for conferring mechanical strength and flexibility. There are commercial binders, such as Nyacol[®] nanoparticles, but in the search for less expensive materials we found that natural ulexite containing borates, such as $\text{NaCaB}_5\text{O}_6(\text{OH})_6 \cdot 5\text{H}_2\text{O}$, are good candidates. It is a cheap and abundant material that can be easily obtained from Argentinean quarries [8].

The preparation of ceramic papers consists of several steps [9], in which the binder particles are incorporated, with filtration being the most critical. To avoid a loss of material during this filtration stage and, thus, favor the retention of the finest particles, especially ulexite particles and ceramic fibers, it is convenient to favor floc formation by neutralization of charges (dual effect of polyelectrolytes) [10]. This is why by determining the charges present after each reagent addition step during the preparation of the ceramic paper, material losses during formation can be avoided or minimized [11,12]. Thus, by taking samples at each intermediate stage of suspension preparation, the charge consumption caused by the addition of each component of the suspension can be obtained, which is related to the type of surface charge of the polyelectrolytes.

In this framework, the aim of this work is to study in depth both the synthesis procedure and the properties of catalytic ceramic papers obtained using ulexite as a binder, in order to improve both the mechanical and catalytic properties of these materials. For this purpose, a battery of characterization techniques is used together with catalytic evaluations for the diesel soot combustion reaction using mixed oxides (Co,Ce and Co,Ba,K) as active materials impregnated in the ceramic papers [13].

2. Results and Discussion

2.1. Optimization of the Mechanical Properties of Ceramic Papers

The influence of the added quantity of binder on the mechanical properties was studied, varying between 2.4, 3.2, and 4 g of purified ulexite per 10 g of ceramic fibers. A detailed study of the amount of charges present in the suspension of the preparation of each paper was also carried out, based on the analysis of samples taken at each intermediate stage of the suspension preparation (Section 3.2.2). The variation of positive charges in the suspension was observed as a function of the added component (Section 2.1.1): polyvinylamine (PVAm), ceramic fibers, ulexite, cellulosic fibers, and polyacrylamide (A-PAM). On the other hand, the percentage of solids retention was also calculated (Section 2.1.2), which is related to the effectiveness of the polyelectrolytes to form flocs and, thus, avoid loss of material through the filter mesh. Finally, the papers with three different amounts of binder were calcined at different temperatures (600, 650, and 700 °C) and then tensile tests were performed for each of the nine samples (Section 2.1.3). In this way, the aim is to select the formulations that generate the optimum values of mechanical properties for the manufacture and application of ceramic papers.

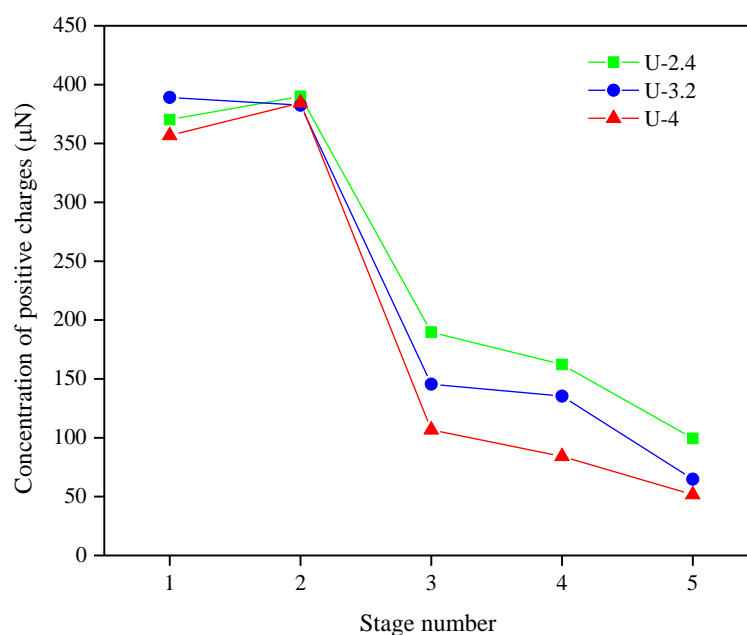
2.1.1. Polyelectrolyte Titrations by Charge-Flow Potential Measurements

Polyelectrolyte titrations were performed on samples extracted from stages 1 to 5, obtained from the suspensions prepared with the three different ulexite contents (U-2.4, U-3.2, and U-4). Table 1 and Figure 1 show the values of positive charges remaining in the suspension after the addition of each reagent. For the titrations, the pH was also measured at the different stages since the charge of the polyelectrolytes is affected by pH.

Table 1. Variation of the concentration of positive charges ($\mu\text{eq.L}^{-1}$) with the addition of the suspension components.

Stage Number	Components	pH	Concentration of Positive Charges ($\mu\text{N} = \mu\text{eq.L}^{-1}$)		
			U-4 *	U-3.2 *	U-2.4 *
1	NaCl + PVAm	7	357	389	370
2	+Ceramic fiber	7	385	382	390
3	+Natural ulexite	9.5	107	146	190
4	+Cellulosic fiber	9.5	84	135	162
5	+A-PAM	9.5	63	65	99

* U-X indicates the suspension used for the preparation of ceramic paper with the different amounts of binder (X).

**Figure 1.** Concentration of positive charges (μN) as a function of the components added to the suspension.

Starting with stage 1, the suspension was found to have a concentration of positive charges of approximately $370 \mu\text{eq.L}^{-1}$ (average value of the three preparations U-4, U-3.2, and U-2.4). They come from the addition of the positive polyelectrolyte (PVAm), which is slightly modified by the addition of ceramic fibers in stage 2. The greatest decrease in the concentration of positive charges is observed with the addition of ulexite (Figure 1, stage 3), which consumes approximately 72% of the charges present in the suspension for the sample with the highest amount of binder (4 g), 62% when adding 3.2 g and 50% for the suspension with 2.4 g of ulexite, which is to be expected since most natural compounds have negative surface charges. Then, with the addition of cellulosic fiber (stage 4), the excess of positive charges continues to decrease, as occurs with the subsequent addition of the anionic polyelectrolyte (A-PAM), in stage 5. It is worth mentioning that the addition of the binder causes an increase in pH from 7 to 9.5, which is maintained in the forming machine. This pH increase causes the decrease in the positive charges conferred by the PVAm, which behaves as a weak polyelectrolyte. To calculate the charges consumed by the pH variation, the sample extracted from stage 2 was brought to pH 9.5 and with the titration it was observed that the charge consumed by pH increase is 20% of the charges consumed between stages 2 and 3. At the end of the preparation, in the sample extracted from stage 5 almost $100 \mu\text{eq.L}^{-1}$ is reached for the sample with 2.4 g of ulexite, while for the other two samples a final positive charge approximately equal to $63 \mu\text{eq.L}^{-1}$ is obtained.

On this basis, it can be concluded that although the 0 loading point is not reached, the final values detected are quite close to the detection limit of the Chemtrac equipment

(in the three analyzed cases of suspensions prepared with different amounts of ulexite). This would indicate that the polyelectrolytes were added in adequate amounts to the preparation, which would allow the formation of flocs and consequently favor the retention of the components added to the suspension, in the filtration stage in the paper forming machine, thus favoring the final structure of the ceramic paper.

However, it is convenient to consider that these studies are indicative but not conclusive due to the physicochemical complexity of the system since the suspension used in the paper forming machine contains electrolytes, particles and two types of polyelectrolytes, and in addition to interactions involving charges, polyelectrolyte rolling and bridging effects may occur.

2.1.2. Retention of Inorganic Solids

To perform an analysis of the loss of material during the manufacturing process of ceramic papers, the ratio between the mass of inorganic solids added to the suspension (since the organic components are completely burned in the calcination stage) and the final mass of the ceramic paper obtained after calcination must be calculated. This is calculated according to:

$$\% \text{ Solids retention} = \frac{\text{mass of ceramic paper} \times 100}{\text{mass of inorganic components added in suspension}}$$

where:

$$\text{mass of inorganic components added in suspension} = \text{mass of ceramic fibers} + 0.754 \times \text{ulexite mass}$$

The factor applied to the mass of ulexite is considered to refer the mass added to anhydrous mass, since when ulexite is calcined at high temperatures, it suffers a mass loss of 24.6% due to dehydrations and transformations typical of this type of borate [8].

Table 2 shows the retention values obtained for each of the nine samples under study, also including the data obtained for a ceramic paper prepared without the addition of a binder (U-0-650). In general, when the binder is added, values of material retention percentages very close to each other are observed, with the best values being obtained for ceramic papers calcined at 650 °C.

Table 2. Retention of inorganic solids in the elaboration of ceramic papers.

Sample	Mass in Suspension [g]	Mass of Ceramic Paper [g]	Solids Retained [%]	Average of Solid Retained [%]
U-2.4-600	11.81	9.76	82.64	
U-2.4-650	11.81	9.83	83.24	82.79
U-2.4-700	11.81	9.74	82.50	
U-3.2-600	12.41	10.36	83.44	
U-3.2-650	12.41	10.40	83.81	82.87
U-3.2-700	12.41	10.10	81.37	
U-4-600	13.02	10.57	81.21	
U-4-650	13.02	10.75	82.62	81.57
U-4-700	13.02	10.53	80.90	
U-0-650	10	9.62	96.17	96.17

Considering the values listed in Table 2 (retention) with the values obtained from the potentiometric titrations (Table 1 and Figure 1), it is concluded that there are no differences in the retention percentages when different amounts of ulexite are incorporated (according to the similar content of the resulting loads at the end of the preparation, stage 5). This indicates that although the amounts of polyelectrolytes and other suspension components

used were adequate, there are other factors that affect to a greater extent the retention of inorganic materials in the final structure of the ceramic paper.

By analyzing the high retention of the paper without binder addition, it can be inferred that the material lost in the filtration stage (inside the forming machine) is mainly composed of natural ulexite, due to the particle size of both the ulexite rods (diameter $< 5 \mu\text{m}$) and the impurities that persist after ulexite purification [8]. Nevertheless, the high retention of ceramic fibers is noteworthy, highlighting the suitability of the dual polyelectrolyte method for the preparation of ceramic papers.

2.1.3. Mechanical Testing of Ceramic Papers with Different Binder Quantities and Calcination Temperatures

Figure 2 shows the curves obtained from the tensile tests, from which the tensile indices (TI) and elastic modulus (EM) were calculated, which are presented in Table 3 for each paper formulation performed. Each curve in Figure 2 is divided into two zones, an elastic zone, characterized by an initial slope and a final declining curve, passing through a maximum that corresponds to the maximum breaking load. The lower the initial slope, the more flexible the paper.

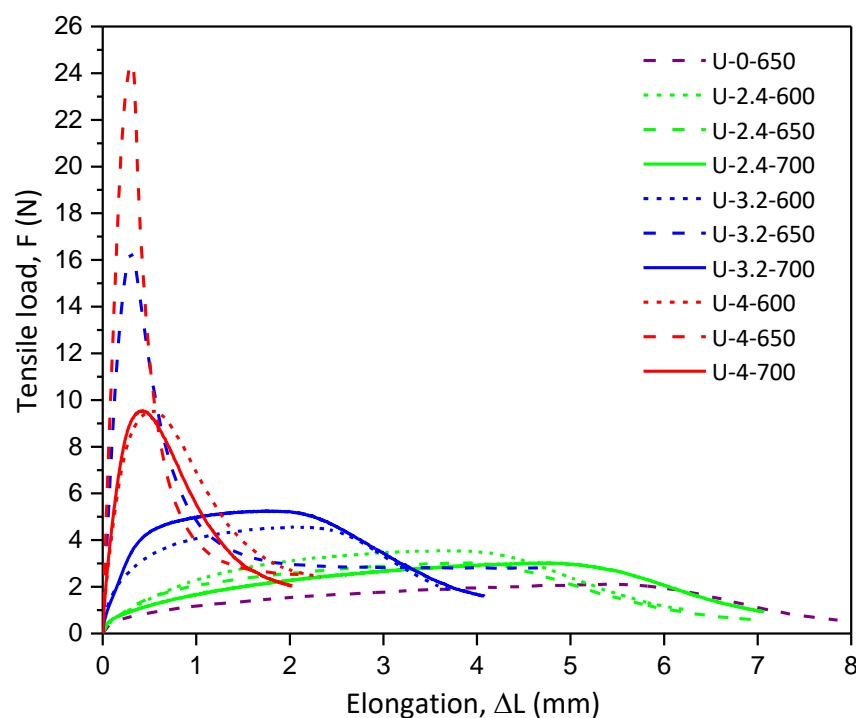


Figure 2. Strength vs. elongation when varying the aggregate amount of binder and calcination temperature.

Table 3. Tensile index and elastic modulus values of ceramic papers prepared with natural ulexite.

Nomenclature	TI (N.m.g^{-1})	EM (MPa)
U-0-650	0.09 ± 0.02	0.76 ± 0.19
U-2.4-600	0.15 ± 0.01	1.38 ± 0.23
U-2.4-650	0.13 ± 0.01	0.75 ± 0.24
U-2.4-700	0.13 ± 0.02	0.53 ± 0.18
U-3.2-600	0.18 ± 0.03	2.46 ± 0.41
U-3.2-650	0.67 ± 0.04	27.43 ± 3.47
U-3.2-700	0.22 ± 0.03	2.76 ± 0.96
U-4-600	0.38 ± 0.04	11.37 ± 2.42
U-4-650	0.96 ± 0.03	36.52 ± 2.67
U-4-700	0.39 ± 0.01	17.23 ± 3.45

Starting with the papers prepared with 2.4 g of ulexite, it is observed that the curves show a very low initial slope (low values of elastic modulus), so that these papers were flexible, but with a low tensile strength (low values of tensile indexes). Furthermore, no significant differences were found between the samples calcined at different temperatures. For comparison, the values of TI and EM for the ceramic paper prepared without the addition of binder is also included and no significant differences are observed in mechanical properties when adding (or not) 2.4 g ulexite.

Considering the papers with 3.2 g of binder, an increase in the tension index is observed for the samples calcined at different temperatures, as well as a lower elasticity, highlighting that at 650 °C the most resistant papers were obtained. A similar behavior is reported by Cecchini et al. when studying papers with anhydrous ulexite calcined at different temperatures, finding a temperature optimum from which the tension index decreases due to excessive softening of the binder, which causes the anhydrous ulexite to cover the ceramic fibers and not form bonding points between them [14]. Similar behavior was found for samples prepared with 4 g of binder. In this case, the ceramic papers showed higher tensile strength values, being able to support loads of up to 24 N.

On the other hand, these results are consistent with the higher amount of retained material obtained in the ceramic paper prepared with 4 g of ulexite (Table 2), since the higher the amount of retained binder, the higher the number of bonding points of ceramic fibers, which helps to increase the mechanical strength. On the other hand, the high elastic modulus obtained for U-4-650 indicates that these papers have extreme stiffness, which makes them brittle, making them difficult to handle and therefore to apply.

For this reason, analyzing the set of parameters evaluated and considering the future applications of ceramic papers, the ceramic paper U-3.2-650 was selected, since it presented a high tensile strength with adequate flexibility for handling.

2.2. Characterization

2.2.1. Ceramic Paper

As was observed in the mechanical tests, the tensile strength due to the action of the binder decreases at temperatures above 650 °C. In order to find an explanation for this behavior, samples of natural ulexite were calcined at 600, 650, and 700 °C and observed under an optical microscope, obtaining the images shown in Figure 3.

It can be observed that uncalcined ulexite has a fibrous morphology, which favors its deposition on the ceramic fibers. When calcined at 600 °C or 650 °C these fibers begin to soften, although they continue to partially maintain the fibrous structure. In the sample calcined at 700 °C it was observed that the ulexite particles completely lose their morphology and melt, which leads to a decrease in their volume. The latter may be the reason for the decrease in the tensile strength of the ceramic papers prepared with ulexite and calcined at 700 °C, since the ulexite could form very small agglomerates that would not be able to bind the ceramic fibers.

On the other hand, by thermogravimetric analysis (TGA-SDTA) it was observed that natural ulexite shows a significant mass loss up to 550 °C together with endothermic recrystallization processes [8], while the anhydrous ulexite studied in previous works [14] did not exhibit mass loss or recrystallized up to 900 °C.

On the other hand, the ceramic papers, both uncalcined and calcined at different temperatures, were analyzed by SEM and EDX to determine through morphology and composition the way in which the ulexite is distributed on the fibrous matrix.

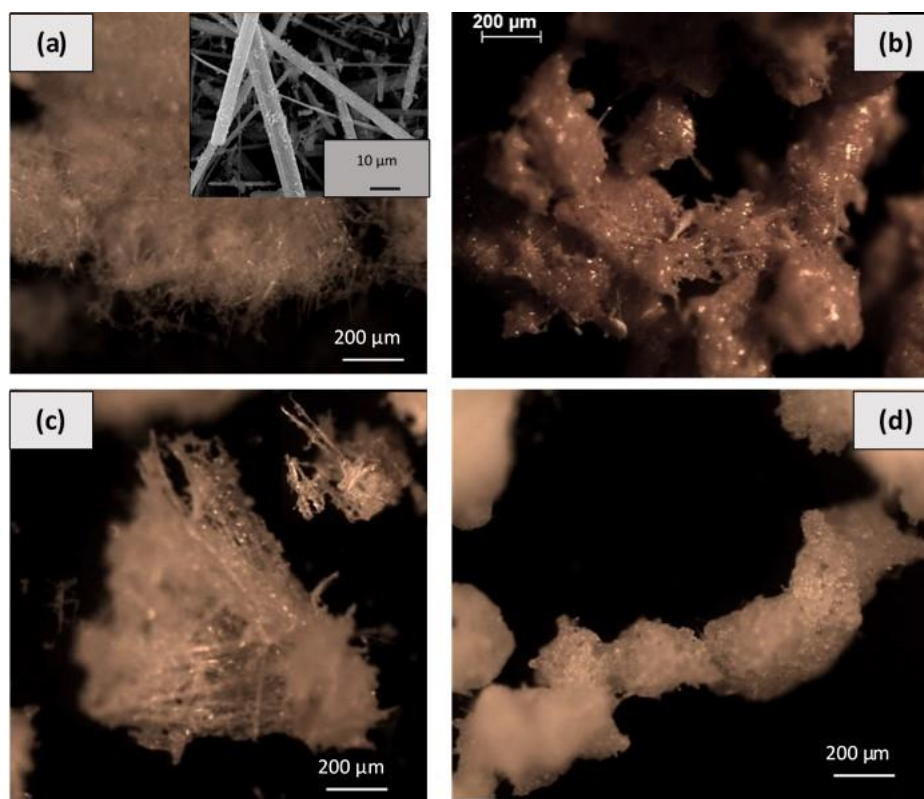


Figure 3. Optical microscope photos of natural ulexite: (a) uncalcined, (b) calcined at 600 °C, (c) calcined at 650 °C, and (d) calcined at 700 °C. Inset: SEM image of natural ulexite fibers.

Figure 4a shows the micrographs of uncalcined ceramic paper where the cellulosic fibers in the form of 40 μm wide ribbons, the ceramic fibers with cylindrical geometry of between 5 and 6 μm in diameter and the ulexite fibers with the form of square-based prisms (4 × 4 μm), 500 μm length, can be distinguished (see also inset Figure 3). By EDX analysis (Figure 5a and Table 4) two points were observed, 1 and 2. For point 1, a higher Si than Al content was obtained, which could correspond to SiO₂ impurities remaining from the ulexite purification treatment, while for point 2 the amounts of Si and Al are similar, which would correspond to typical proportions coming from ceramic fibers. Impurities of Mg, K, and Fe, typical of ulexite obtained directly from quarries, were also detected. It should be taken into account that even after several purification stages have been carried out, there are still some impurities remaining from the quarried material, mainly silica.

Table 4. EDX analysis of ceramic papers calcined at different temperatures (Figure 5).

Element	Sample							
	Uncalcined		Calcined at 600 °C		Calcined at 650 °C		Calcined at 700 °C	
	Point 1	Point 2	Point 1	Point 2	Point 1	Point 2	Point 1	Point 2
O	75.7	77.2	70.6	74.7	72.0	73.4	69.9	66.7
Si	10.4	9.7	7.3	10.6	9.3	6.7	13.0	11.9
Al	3.3	9.1	11.3	10.6	8.5	8.2	7.0	9.3
Ca	0.9	-	5.2	5.5	4.7	8.0	0.6	2.4
Na	-	-	0.3	-	1.1	-	1.1	1.1
Mg	7.9	2.3	0.6	-	3.6	2.0	7.1	3.7
B	-	-	1.1	2.3	-	0.9	-	1.0
N	-	-	3.7	-	-	-	-	-
Fe	1.7	0.3	-	-	0.4	0.4	0.9	0.9
K	-	1.3	-	-	0.3	0.2	0.3	0.3

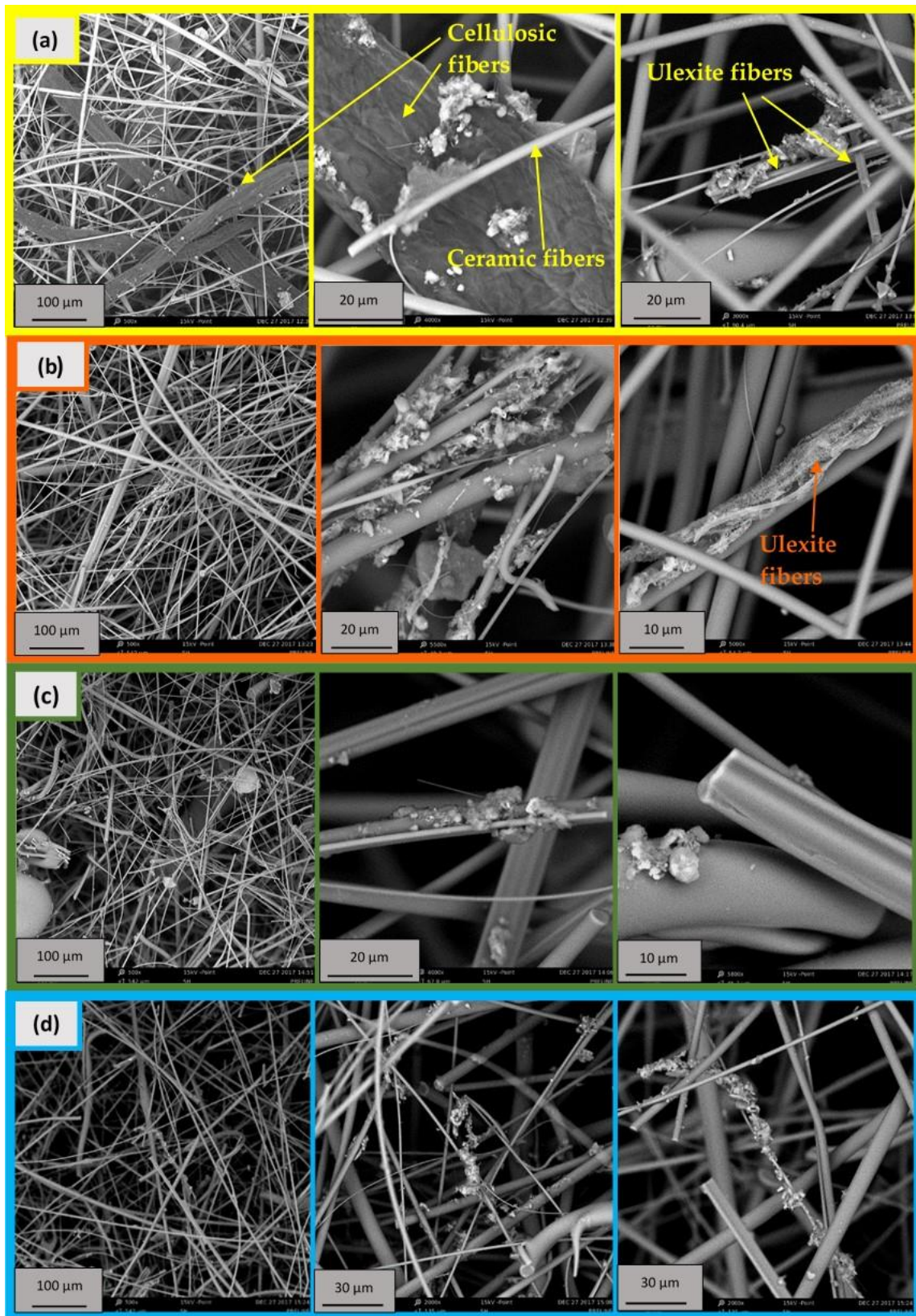


Figure 4. SEM micrographs of ceramic papers prepared with 3.2 g of ulexite, uncalcined and calcined at different temperatures: (a) U-3.2, (b) U-3.2-600, (c) U-3.2-650, and (d) U-3.2-700.

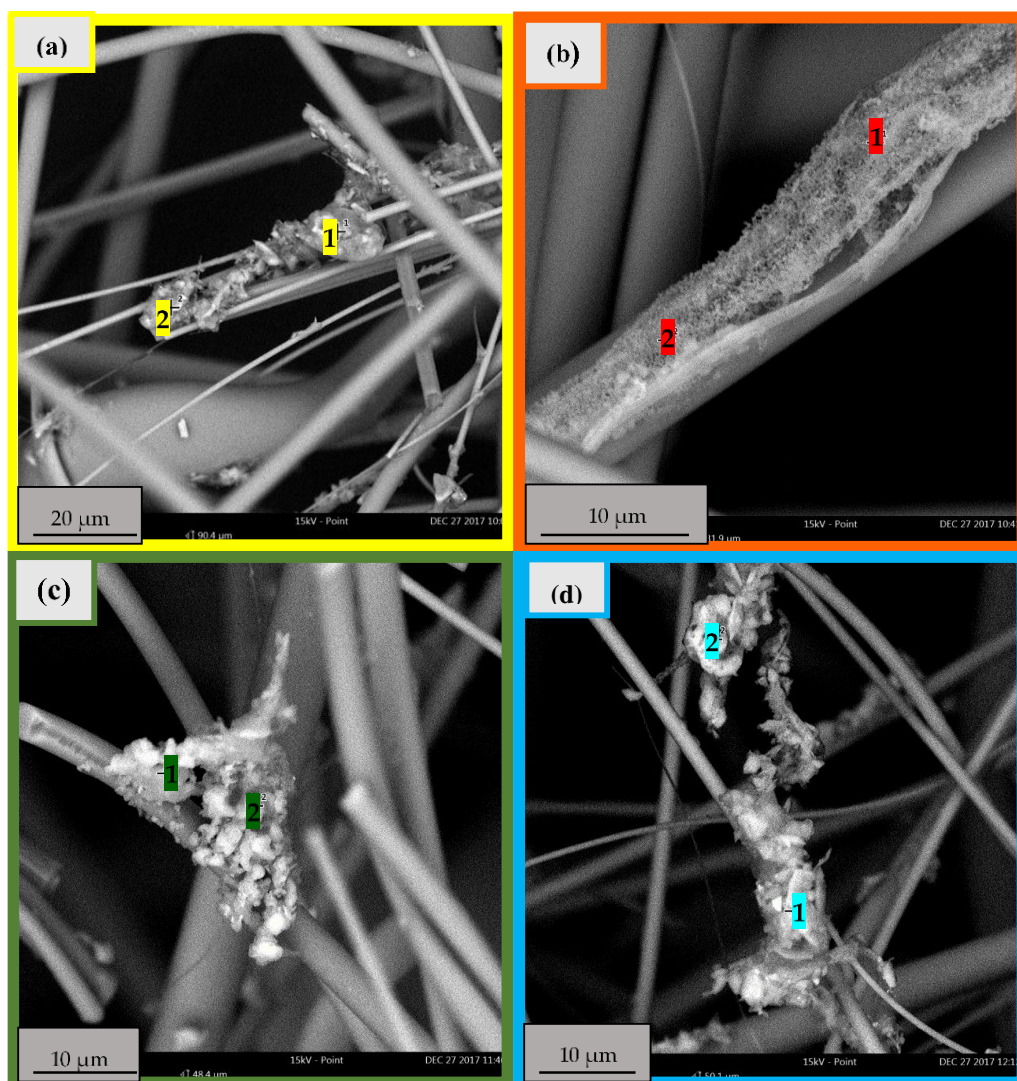


Figure 5. SEM-EDX spot analysis of uncalcined and calcined ceramic papers at different temperatures: (a) U-3.2, (b) U-3.2-600, (c) U-3.2-650, and (d) U-3.2-700. Numbers indicate the zones where EDX spectra were acquired.

Figure 4b, corresponding to the micrographs taken for the ceramic paper calcined at 600 °C, shows a lattice of ceramic fibers together with deposits of material on them. The absence of cellulosic fibers (removed by calcination) is evident. At higher magnification, a variety of semi-molten and agglomerated structures deposited on the ceramic fibers, formed during calcination, can be observed, which could correspond to natural ulexite since it begins to soften at this temperature. In order to corroborate this, in the analysis performed by EDX (Figure 5b) on the semi-softened fiber seen by SEM, elements, such as B, Ca were detected, which confirms that they were deposits of ulexite, which partially softens at 600 °C as observed by optical microscopy (Figure 3b). In point 2, the atomic ratios of Al and Si correspond to the presence of ceramic fibers.

In the micrographs of the ceramic papers calcined at 650 °C (Figure 4c), semi-molten fibers (with more rounded edges) are observed, which, due to their geometry, could correspond to natural ulexite, or to the union of ceramic fibers (cylindrical) due to the softening of the binder. By EDX (Figure 5c), deposits were observed joining the ceramic fibers that correspond to the binder since the elements Ca and B were detected, in addition to Si and Al in proportion corresponding to the ceramic fibers.

Finally, in the SEM micrographs of the ceramic papers calcined at 700 °C (Figure 4d), small deposits are observed on the fibers that do not achieve fiber bonding but are spread heterogeneously. EDX spot analysis of these deposits (Figure 5d) indicated the presence of ulexite mixed with impurities of Si, Mg, K, and Fe from the quarry.

2.2.2. Catalytic Ceramic Paper

Analyzing the results of the mechanical properties, the papers with 3.2 g of ulexite and calcined at 650 °C were chosen for the incorporation of the active phases, since with this amount of binder and calcination temperature adequate values of tensile index and elastic modulus were obtained. The BET surface area of the ceramic paper (U-3.2-650) was 14 m²/g. Two combinations of catalytic elements, Co,Ce and Co,Ba,K were used, since both systems have been studied in the working group and found to be active for diesel soot combustion [9]. The catalysts were incorporated to the ceramic paper (U-3.2-650) by dropwise impregnation of mixed solutions of the catalytic precursors, followed by calcination at 600 °C to obtain 5, 12, and 24 % *w/w* of total active phase with respect to the mass of the ceramic paper. The papers thus obtained were named Co,Ce(x)U-I and Co,Ba,K(x)U-I, where x indicates the % *w/w* of active material incorporated.

After adding the catalytic phases, different analysis techniques (SEM, EDX, and XRD) were used to determine the distribution of the catalyst on the surface of the fibers composing the ceramic paper and to identify the species present after the second calcination.

In the lower magnification, SEM micrographs (Figure 6) for the Co,Ce(5)U-I and Co,Ba,K(5)U-I samples, the distribution of the active phase on the fiber lattice is observed. In a more detailed view, it can be seen that in the potassium containing sample (Co,Ba,K(5)U-I) the catalyst is distributed at the fiber junctions and between the fibers, while for Co,Ce more compact agglomerates are found deposited around each ceramic fiber.

For the identification of the different types of aggregates, spot EDX analyses were performed on them. Two different zones of the Co,Ce(5)U-I sample were analyzed: one with a large catalytic aggregate (>10 µm) shown in Figure 7a and another with deposits on a fiber, shown in Figure 7b. Figure 7a shows the spectra at 4 points, where at points 1 and 2 the presence of Ca, a constituent of ulexite, is observed together with Co and Ce signals, showing that the active phase is preferentially deposited on the binder. In contrast to this, in points 3 and 4 intense Si and Al signals are observed, coming from the SiO₂-Al₂O₃ ceramic fibers. It can be observed that in point 2 Si was also detected in high proportion, which would be associated with SiO₂ impurities coming from the binder, since the Al signal is much less intense. Figure 7b shows deposits of circular geometry (coin type) distributed on the ceramic fiber which are mainly composed of Co (point 1) and fibrous formations that could correspond to the binder since the amount of Ca increases in these formations (point 2). In all cases, in greater or lesser proportion, Si and Al signals are observed, coming from the ceramic fibers.

When performing the spot analysis on the Co,Ba,K(5)U-I sample, it is observed that the catalyst is deposited on the fibers according to two very different types of morphologies. Figure 8a shows a large catalytic deposit joining several ceramic fibers, with the appearance of a “molten material” (as observed by SEM) and 4 points were analyzed. Although the presence of potassium is evident in all the analyzed points, it can be seen that on the “molten” part the proportion of K is higher (points 1 and 3), and, in general, the K signal is accompanied by the Ca signal, through which the binder is identified. On the other hand, the deposits with higher brightness and more defined shape could be identified as Ba-containing particles. Finally, Co seems to be in the same proportion in all the analyzed points, which implies that it has a good distribution both on the binder and on the fibers. Figure 8b shows filament growths perpendicular to the fibers of approximately 3 µm. When EDX analysis was performed on the three marked points, the presence of barium was found in all cases. In addition, on the filaments (points 1 and 2) the presence of calcium corresponding to natural ulexite can be detected and at the base of these filaments the proportions of Co and K increase (point 3).

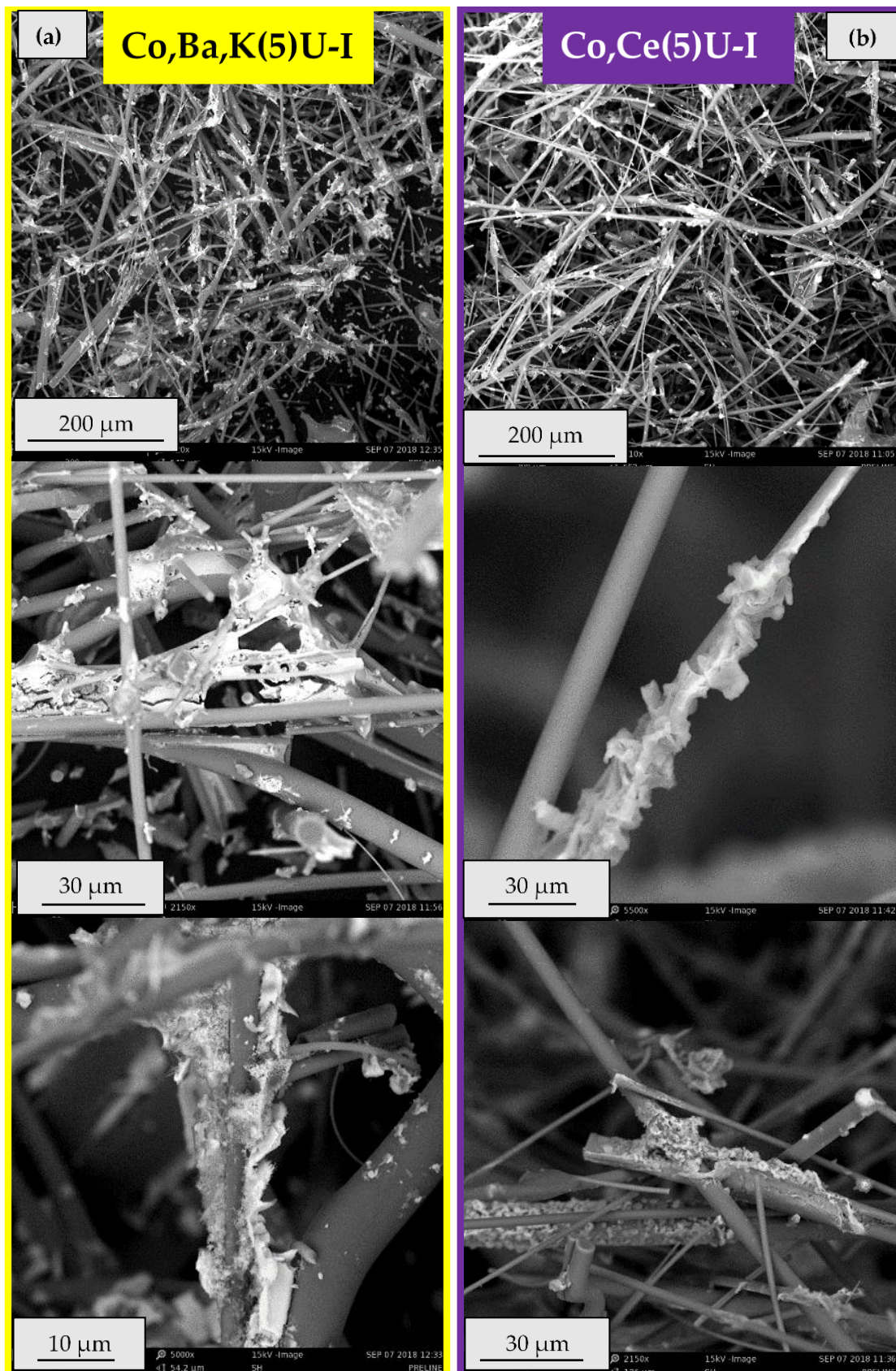


Figure 6. Morphology of catalytic ceramic papers with 5% active phase (a) Co,Ba,K(5)U-I and (b) Co,Ce(5)U-I.

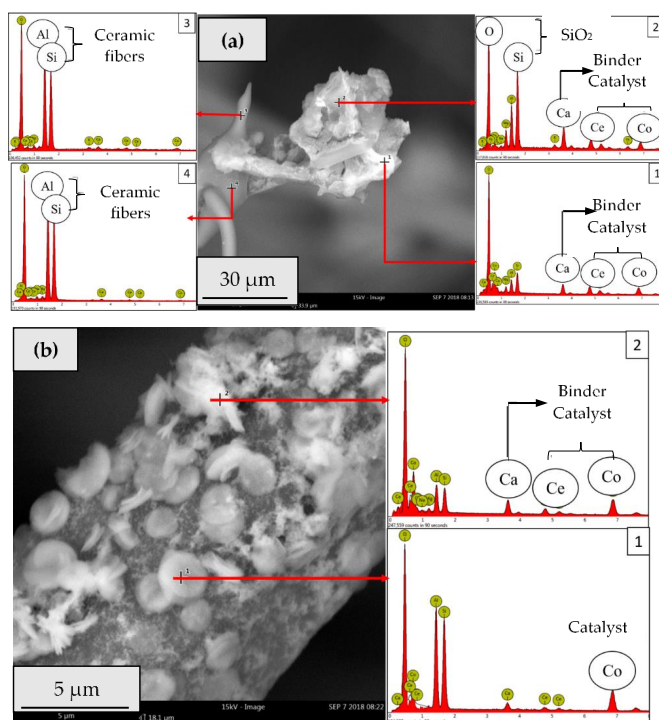


Figure 7. Spot EDX analysis for the identification of catalytic deposits for the sample Co,Ce(5)U-I. (a,b) are different analyzed zones of the sample.

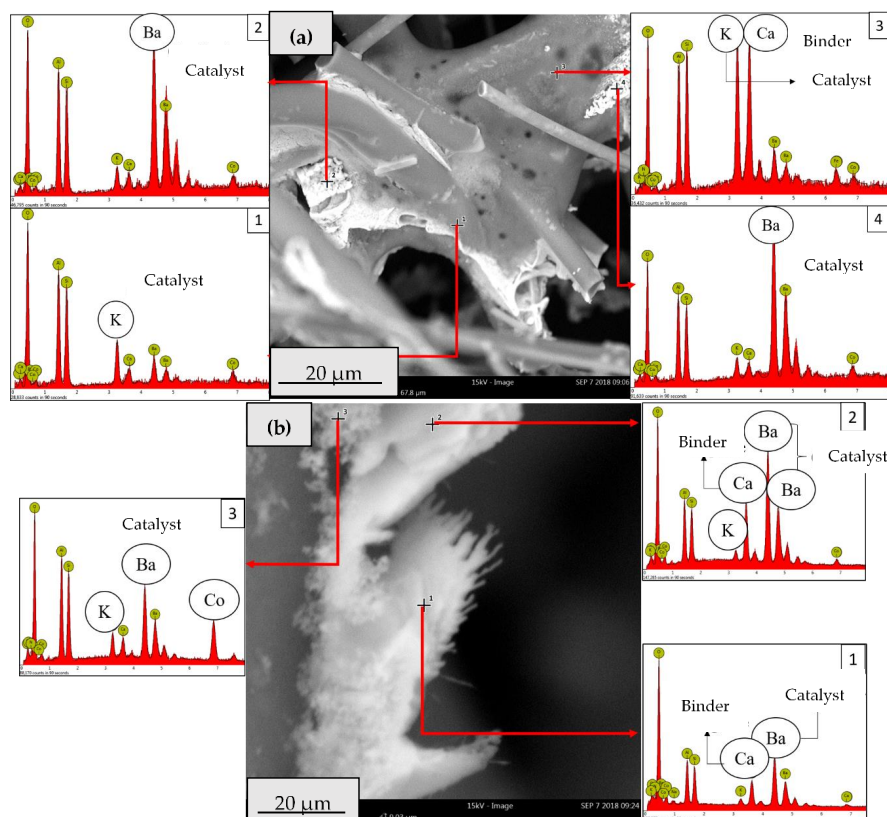


Figure 8. Identification of the deposits found for the sample Co,Ba,K(5)U-I by spot EDX analysis. (a,b) are different analyzed zones of the sample and numbers indicate different points where EDX spectra were acquired.

2.3. Catalytic Activity Relationship with Composition/Morphology of Catalytic Ceramic Paper

Temperature programmed oxidation (TPO) experiments of diesel soot were carried out using the catalytic ceramic papers with 5, 12, and 24% catalytic phase. In addition, a sample of ceramic paper without the added catalyst (U-0-650) was evaluated in order to analyze how the substrate behaves alone in reaction. It was found that 5% total active phase with respect to the mass of ceramic paper did not yield good results, since a maximum soot burning rate (T_M) temperature was obtained at 500 °C and 560 °C for the Co,Ba,K(5)U-I and Co,Ce(5)U-I samples, respectively (Figure 9a,b). In the case of the non-catalytic paper, the T_M obtained was 530 °C, so with the addition of this amount of catalyst it was not possible to confer catalytic activity to the ceramic papers. Regarding the evaluations of the ceramic papers with a greater amount of active phase shown in Figure 9, it is observed that a greater amount of active phase incorporated improves notably the activity of the ceramic papers with ulexite. For the sample containing Co,Ce, when the amount of active phase was increased to 12%, a T_M of 440 °C was obtained, reaching 410 °C with 24% of catalyst incorporated (Figure 9a). Although for the system containing Co,Ba,K, with 12% of the catalytic phase incorporated, a T_M of 410 °C was obtained and no difference was observed when the amount of catalyst was doubled (Co,Ba,K(24)U-I, Figure 9b).

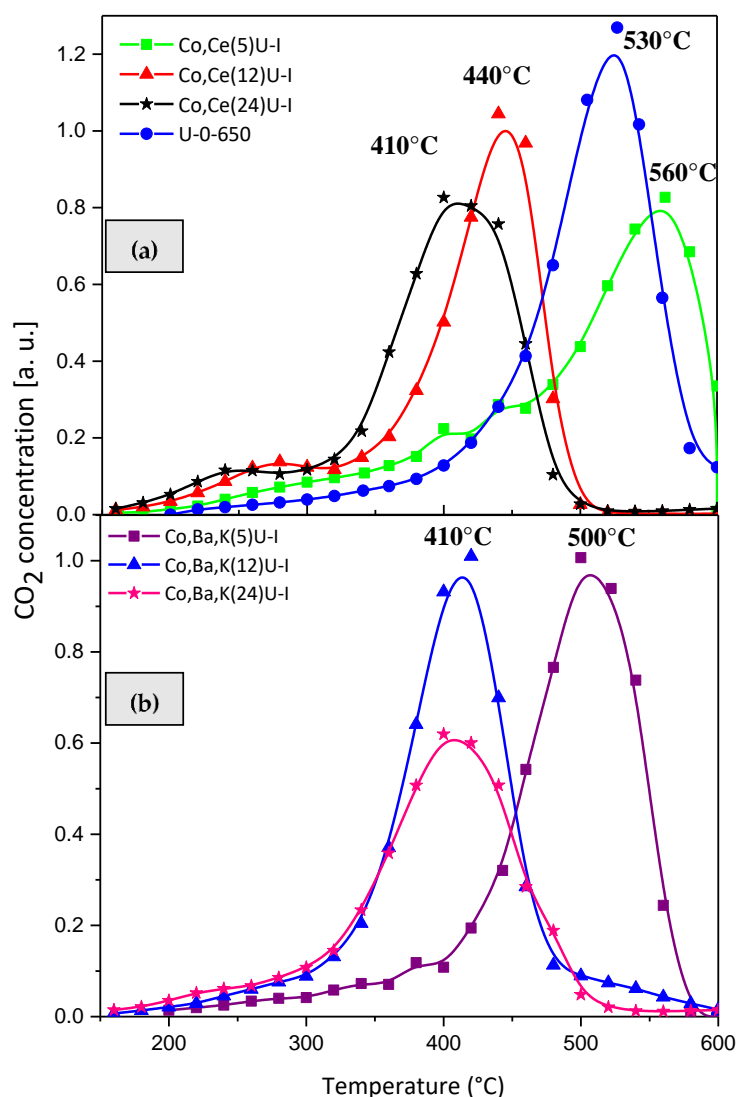


Figure 9. Effect on the catalytic activity for diesel soot combustion of the catalyst content in ceramic papers with ulexite containing: (a) Co,Ce and (b) Co,Ba,K.

In order to analyze the cause of the improvement of the catalytic activity with the increase in the amount of active phase, X-ray diffraction was performed on the samples with 5 and 12% of catalyst incorporated. As can be seen in Figure 10, for both Co,Ce(12)U-I and Co,Ba,K(12)U-I, increasing the amount of active phase results in more intense peaks in the diffraction patterns of the samples, indicating an increase in the crystallinity of the species found: Co_3O_4 (JCPDS-ICDDD # 42-1467) and CeO_2 (JCPDS-ICDD # 34-394) for systems with Co, Ce and Co_3O_4 (JCPDS-ICDDD # 42-1467), and BaCO_3 (JCPDS-ICDD # 45-1471) for systems with Co, Ba, and K.

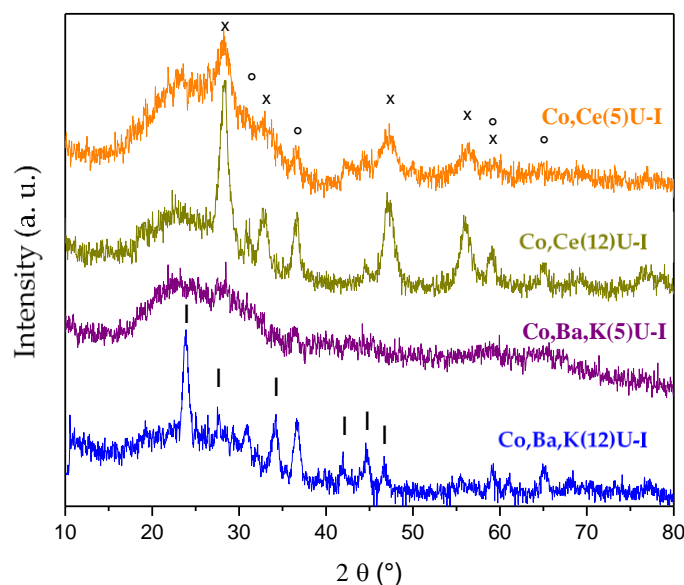


Figure 10. XRD diffraction patterns of catalytic ceramic papers with natural ulexite and with Co,Ce and Co,Ba,K addition. Symbols (°) Co_3O_4 , (x) CeO_2 , and (I) BaCO_3 .

On the other hand, and with the aim of studying a possible partial encapsulation of the catalyst, as observed in previous works when incorporating zeolites in ceramic papers with borates as binders [15], the SEM micrographs (Figure 6) and EDX composition results of the systems with 5% *w/w* were compared with the SEM micrographs of papers with 12% *w/w* of active phase (Figure 11). The increase in catalyst content is evidenced, which is distributed covering the ceramic fibers in higher proportion compared to the samples containing only 5% *w/w* of active phase (Figure 6). In particular, for the sample Co,Ce(12)U-I (Figure 11a) isolated agglomerates continue to be observed, leaving sections of ceramic fibers uncoated, so the improvement in catalytic activity may be due to a greater amount of catalytic clusters compared to the sample containing only 5% *w/w*. On the other hand, for the sample Co,Ba,K(12)U-I (Figure 11b) a complete coverage of the ceramic fibers by the catalyst is observed. A new morphology of the catalytic deposits was also found in the form of oval particles approximately 10 to 12 μm long, which are found in large quantities and distributed throughout the fibrous matrix (Figure 11b). Finally, it is observed in Figure 11b (higher magnification image) that with 12% *w/w* of catalyst, the ceramic fiber is totally and homogeneously covered by small particles, which explains that only 12% *w/w* of active phase reaches the optimum catalytic activity for this system (Figure 9b). In addition, to identify the new morphologies observed, point EDX was performed on them (Figure S1) and it was determined that the oval particles are mainly composed of barium, i.e., the BaCO_3 (identified by XRD) would no longer be growing in the form of filaments perpendicular to the fibers, as was found in the Co,Ba,K(5)U-I samples. It can also be observed that the smaller particles homogeneously distributed homogeneously coating the ceramic fibers are mainly composed of Co and have a size of 1 to 2 μm .

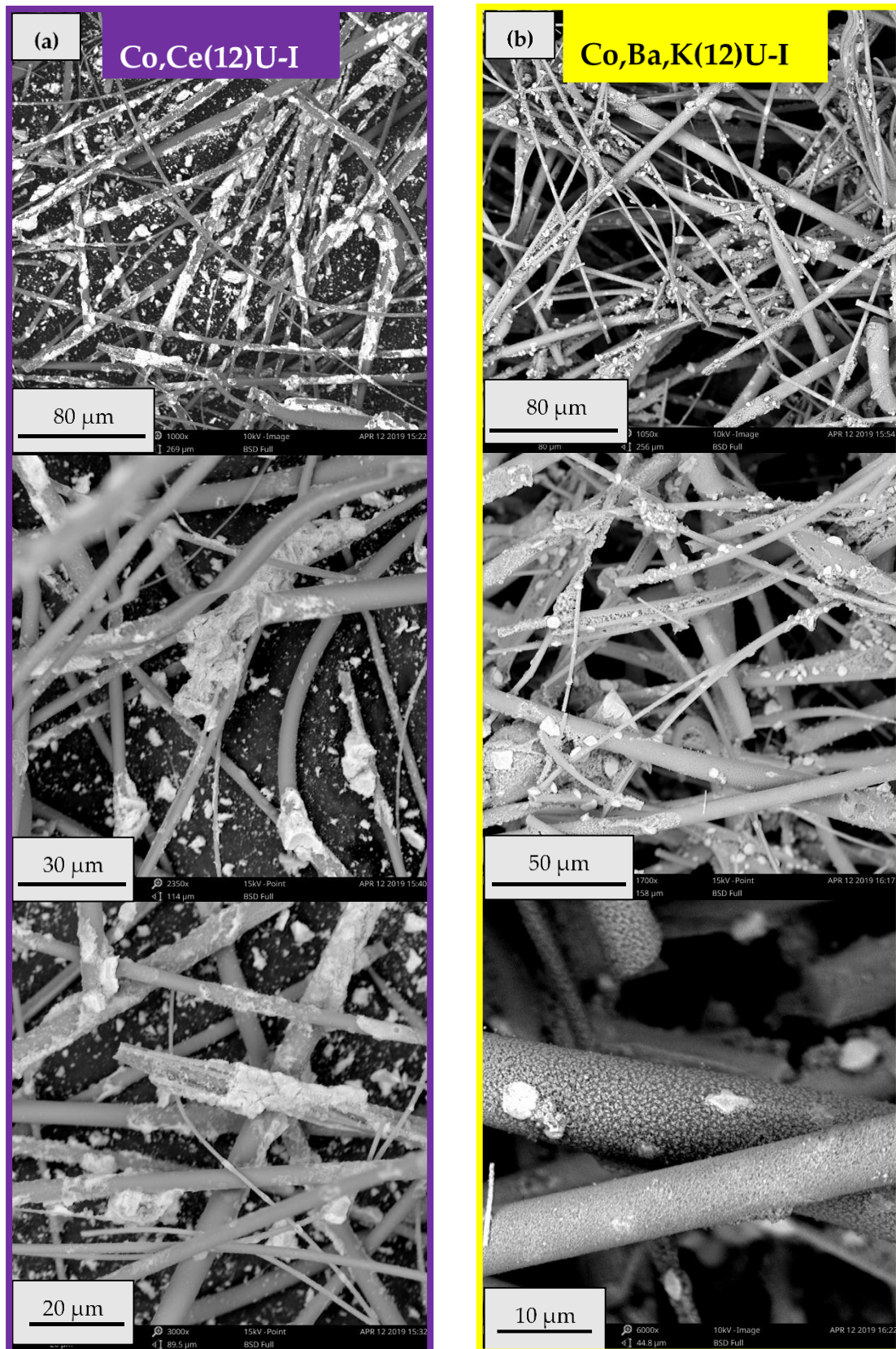


Figure 11. SEM micrographs of the samples with 12% active phase: (a) Co,Ce(12)U-I and (b) Co,Ba,K(12)U-I.

Table 5 shows a comparison of the activity results obtained in this work with others reported in the literature. T_M values are close to the best catalysts showed in the table, and comparing among those that use ceramic paper as support, the mechanical properties of that using ulexite as the binder (this work) are better than the reported in a previous one using commercial Ce Nyacol.

Table 5. Catalytic activity compared with selected catalysts reported for soot combustion.

Catalyst/Support	T_M (°C)	Oxidizing Flow	References
Co,Ba,K/CeO ₂	370	4% NO + 18% O ₂	[16]
Co,Ba,K/ α -Al ₂ O ₃	450	Air	[17]
Co,Ba,K/ZrO ₂ /Metallic foam	380	0.1% NO + 18% O ₂	[18]
Co,Ba,K/ceramic paper ^a	390	0.1% NO + 18% O ₂	[9]
Co,Ba,K/ZrO ₂ /Cordierite monolith	400	0.1% NO + 18% O ₂	[19]
Co,Ce/ceramic paper ^a	480	0.1% NO + 18% O ₂	[9]
Co,Ce/Ni nanosheet	430	600 ppm NO + 10% O ₂	[20]
K/MnO ₂	490	10% O ₂	[21]
Pt/LaCoO ₃	393	Air	[22]
Co,Ba,K/ceramic paper ^b	410	0.1% NO + 18% O ₂	[this work]
Co,Ce/ceramic paper ^b	440	0.1% NO + 18% O ₂	[this work]

^a Ceria nanoparticles (Nyacol) were used as binder. ^b Ulexite materia was used as binder.

3. Materials and Methods

3.1. Conditioning of Materials to Be Used in the Preparation of Ceramic Papers

3.1.1. Binder Conditioning

The boron compound used as a binder was extracted from the mineral ulexite (NaCaB₅O₆(OH)₆·5(H₂O)) from a quarry in northern Argentina by the company BORAX. The extracted mineral has a variety of impurities composed mainly by silica (SiO₂), which was separated by an elutriation method. To do this, the extracted material is first sieved with an 80 mesh sieve, collecting the finest particles that pass through the sieve. Then, the sieved sample is poured into an Erlenmeyer, distilled water is added and sonicated for 15 min. Then, it is left to rest, the supernatant is recovered and the decanted silica is discarded. This process is repeated until no sand remains are observed. Finally, the supernatant containing the ulexite is filtered under vacuum and the solid collected in the filter is dried in an oven at 130 °C for 24 h. Purified ulexite is thus obtained, with a process yield of 30%.

3.1.2. Conditioning of Ceramic Fibers

Ceramic fibers were obtained by elutriation from a commercial ASTS brand mat (density 128 g.m⁻³, thickness 2 inches). Fibers were separated from non-fibrous particles by placing 10 g of mat with 2 L of 180 mS conductivity water in a standard L&W disintegrator for 15 min. It was then transferred to a larger container where more water was added, properly conditioned. The particles were allowed to settle and from the supernatant the fibers were obtained by filtration. This process has a yield of 50%. The fibers obtained have a composition of 50% *w/w* SiO₂, 48% *w/w* Al₂O₃, and 2% *w/w* impurities.

3.1.3. Conditioning of Cellulosic Fibers

The cellulosic fibers must be hydrated and separated to achieve a homogeneous distribution of the fibers in the paper mat to be formed. For this, 1.5 g of blotting paper was placed in water for 15 min and then poured into the disintegrator with 2 L of 180 mS conductivity water. The equipment is operated for 4 min and the resulting suspension is then filtered, obtaining the wet disintegrated fibers

3.2. Obtaining Catalytic Ceramic Papers

3.2.1. Papermaking Technique

The ceramic papers were prepared using a standard papermaking method described by SCAN-C 26:76 and SCAN-M 5:76, with some modifications to adapt to the use of ceramic fibers. The paper structuring was carried out by a batch process using a vessel with continuous agitation where 1000 mL of 0.01 N NaCl solution was added to regulate the ionic strength of the medium, 66 mL of cationic polyelectrolyte solution, polyvinylamine (PVA_m) ($1 \text{ g}\cdot\text{L}^{-1}$) and 10 g of purified ceramic fibers. Then, the binder (ulexite in different amounts), 1.5 g of conditioned cellulosic fibers and, finally, 23 mL of anionic polyelectrolyte solution, polyacrylamide (A-PAM) ($1 \text{ g}\cdot\text{L}^{-1}$), were added to consolidate the flocs formed. Each component of the suspension was added after 3 min of constant and moderate agitation to obtain homogeneous size flocs and a good distribution of the components.

The diluted aqueous suspension (Figure 12-1) was uniformly poured into the forming machine (Figure 12-2) filled with water of 180 mS conductivity, homogenized with a standard manual stirrer so as not to break the formed flocs, and then filtered through the 150 mesh filter screen ($100 \mu\text{m}$ aperture). At this point, the drainage capacity of the water is critical, in order to obtain a paper of homogeneous thickness. The wet sheet was removed from the filter mesh and pressed at 367 kPa (Figure 12-3) with a hydraulic press. Pressing is carried out in two stages of 5 and 2 min duration, with the objective of eliminating the highest proportion of water and consolidating the structure of the sheet (Figure 12-4).

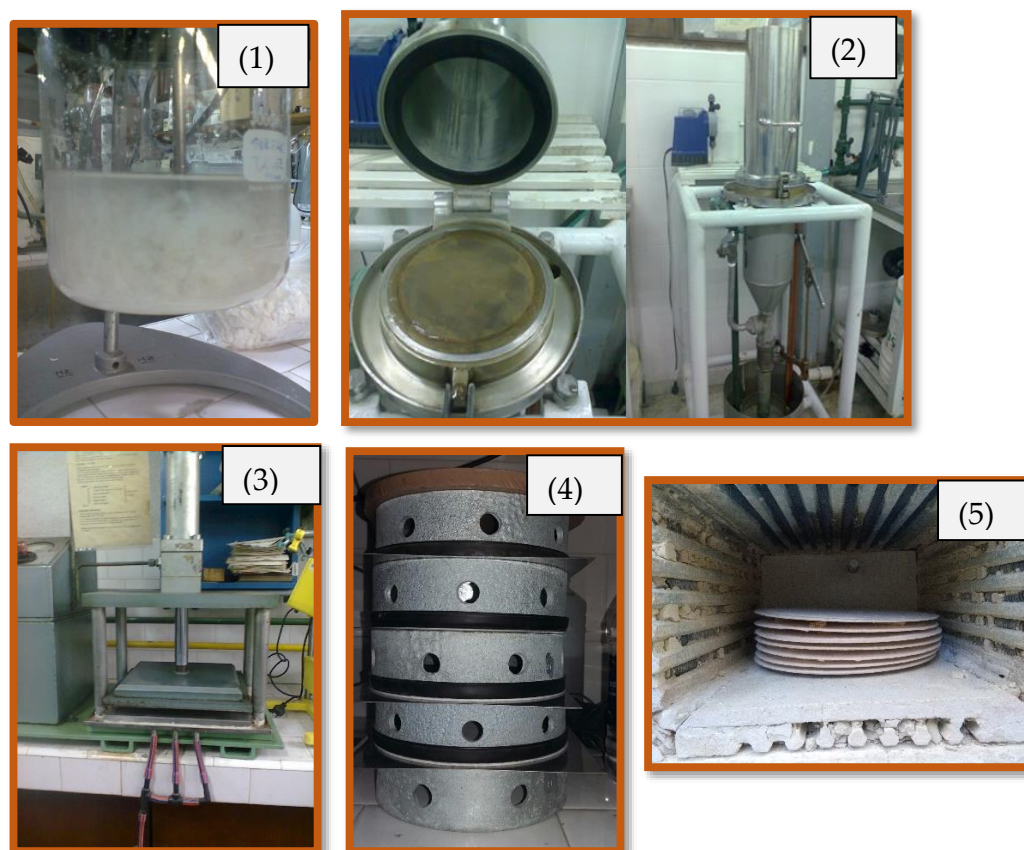


Figure 12. Images of the equipment used in each stage of the production of ceramic papers. (1) suspension of the components of the ceramic paper forming flocs by the action of polyelectrolytes, (2) paper making machine ($100 \mu\text{m}$ filter mesh), (3) hydraulic press, (4) drying in a controlled environment (52% humidity, $22 \text{ }^\circ\text{C}$), and (5) calcination in a muffle.

Finally, it is calcined for 2 h in a muffle (Figure 12-5) with a heating ramp of $1 \text{ }^\circ\text{C}\cdot\text{min}^{-1}$ until the required temperature is reached (different temperatures were evaluated, from

600 °C to 750 °C). In this final stage of paper preparation, the cellulosic fiber is eliminated (since it burns completely between 250 and 330 °C [23]), which confers a high permeability to the paper by producing a highly porous lattice. The result is a paper that generates practically null pressure drop in the presence of a gaseous stream. On the other hand, at this stage, when the binder reaches the softening temperature (between 600 and 750 °C), it generates bonding points between the ceramic fibers, providing mechanical strength to the paper.

The papers thus obtained were denominated U-X-T, where T indicates the calcination temperature and X is the loading in grams of binder: 2.4, 3.2 or 4 (see Table 6). The latter values correspond to 15.3, 19.4 or 23.2% *w/w*, respectively, of anhydrous binder referred to the mass of inorganic components added in the suspension.

Table 6. Formulation of ceramic papers obtained by varying the amount of binder and calcination temperature.

Nomenclature	Natural Ulexite (g)	Calcination Temperature (°C)
U-2.4-600	2.4	600
U-2.4-650	2.4	650
U-2.4-700	2.4	700
U-3.2-600	3.2	600
U-3.2-650	3.2	650
U-3.2-700	3.2	700
U-4-600	4	600
U-4-650	4	650
U-4-700	4	700

3.2.2. Polyelectrolyte Titration by Charge-Flow Potential Measurements

The charge density of the paper preparation suspension was determined by polyelectrolyte titration [24] using charge-flow potential measurements after the addition of each reagent. The titration end point is obtained when the measured potential is 0 mV.

For this purpose, a Chemtrac, USA, streaming current detector (Coagulant Charge Analyzer CCA3100) was used, which has a cylindrical Teflon cup inside which a piston with a vertical oscillating movement at constant frequency moves. The cation of the cationic polyelectrolyte (PVAm) is adsorbed on the piston, leaving the counterion (negative) within the solution. The movement of the piston generates the separation of the charge centers of the anion and the surrounding ionic cloud, which generates a potential difference that is detected by two internal electrodes placed at different heights.

A standard anionic polyelectrolyte, potassium polyvinyl sulfate (PVSK) with a molecular weight of 130 kDa, supplied by AppChem, England, was used as titrant reagent. A solution of 200 µN concentration was prepared. Titrations were carried out at a constant ionic strength (given by a 0.01 N NaCl solution) and at the pH of the suspension corresponding to each component addition step, which ranged from 6.5 to 9.5. The pH measurements were performed with a Thermo scientific Orion Star A111 pH meter.

For the titration, a certain amount of the sample whose charge is to be determined is placed in a 150 mL beaker and the medium is filled with 0.01 N NaCl solution under constant stirring. As the titrant is added from a microburette, the charges are neutralized and the measured potential decreases. The end point of the titration is reached when the sample is completely neutralized and no potential difference is recorded, which corresponds to the zero mV potential value recorded by the Chemtrac instrument.

Sample Preparation for Titration: To determine the amount of positive charge remaining unadsorbed from the cationic polyelectrolyte, the solid phase of the samples must be removed to avoid possible interferences in the determinations. For this purpose, 25 mL samples were extracted, after the addition of each component to the suspension, so that each sample is composed of:

Sample 1: NaCl + PVAm;

Sample 2: NaCl + PVAm + Ceramic Fibers;
 Sample 3: NaCl + PVAm + Ceramic fibers + Natural Ulexite;
 Sample 4: NaCl + PVAm + Ceramic Fibers + Natural Ulexite + Cellulosic Fibers;
 Sample 5: NaCl + PVAm + Ceramic Fibers + Natural Ulexite + Cellulosic Fibers + A-PAM.

The samples were then centrifuged in a ROLCO model 2036 centrifuge for 90 min at 4000 rpm. The solids-free supernatant was then extracted and used for the charge determinations (Figure S2).

3.2.3. Incorporation of the Active Phases

For the addition of catalysts to the ceramic papers obtained, mixed solutions composed of Co,Ba,K and Co,Ce were prepared and used to impregnate both sides of the paper by dripping until saturation. Thus, loads of 5, 12, and 24% *w/w* of total active phase with respect to the mass of ceramic paper were obtained (maintaining in all cases atomic ratios Co:Ba:K = 1:1.33:0.58 and Co:Ce = 1:2.37, respectively). The impregnated papers were oven dried for 1 h at 80 °C and then calcined at 600 °C for 2 h to obtain the corresponding oxides. These systems were named Co,Ba,K(x)U-I and Co,Ce(x)U-I, where (x) indicates the percentage of total active phase added.

3.3. Characterization of Catalytic Ceramic Paper

SEM-EDX. To observe the fiber network and its junctions, as well as the distribution and morphology of the incorporated catalysts, a Phenom scanning electron microscope model Word ProX (Holland), operated under the backscattered electron mode at 15 kV accelerating voltage, was used. The semiquantitative analysis of the elements present in the catalytic ceramic papers was performed with the same equipment, whose results were obtained by the theoretical quantitative method (SEMIQ), which does not standards.

XRD. The detection of crystalline phases for the identification of the catalytic species deposited on the ceramic papers was carried out with a Shimadzu XD-D1 model equipment with monochromator. The characteristics/conditions used were: X-ray tube, CuK α radiation (0.154 nm), copper anode, 30 kV working voltage, 40 mA working current, Ni filter (standard for copper anode), horizontal goniometer (180 mm radius), data acquisition range = 10° to 80° at 1°·min⁻¹, NaI scintillation counter detector, and 9924B photomultiplier.

Stereo microscopy. Observations of the ulexite particles were made to determine the approximate particle size and morphology after calcination at different temperatures. A Leica 2000 Zoom stereo microscope, model S8 APO, which has a digital camera for image capture, was used for this purpose.

Mechanical properties. Two parameters are important for evaluating the handleability of the prepared ceramic papers. On the one hand, the tensile index (IT, Equation (1)), which is related to the maximum force that the sample resists before breaking, and on the other hand, the elastic modulus (EM, Equation (2)), related to the stretching that occurs in the paper up to its breaking point. For the evaluation of these parameters, a universal testing equipment, INSTRON model 3344, with a 1000 N load cell, connected to a PC with INSTRON software for data acquisition, was used. The tests were performed under the TAPPI T 576 pm-07-2007 standard. Samples of 2.5-mm-thick ceramic paper were cut into 5 × 7 cm rectangular probes, placed between grips and subjected to tensile force, from which graphs of tensile load (N) as a function of stretching (mm) were obtained, from which the desired parameters were calculated with the following equations:

$$TI (N \cdot m \cdot g^{-1}) = \frac{F(N)}{G(g \cdot m^{-2}) \cdot W (m)} \quad (1)$$

where F is the maximum breaking load (N), G represents the paper weight (g·m⁻²), and W is the width of the probe (m).

$$EM(MPa) = \frac{10^{-6} \cdot \Delta F (N) / (W (m) \cdot E (m))}{\Delta L (m) / L (m)} \quad (2)$$

where $\Delta F/\Delta L$ ($\text{N}\cdot\text{m}^{-1}$) is the slope in the elastic zone of the curve, E (m) is the thickness of the paper, and L (m) represents the distance between grips.

BET measurements. Nitrogen adsorption–desorption isotherms were obtained at -196 °C on a Quantachrome Autosorb 1C instrument. Previously, samples were out-gassed at 350 °C for 2 h under vacuum. The Brunauer–Emmett–Teller (BET) equation was used for calculating the specific surface area of the ceramic paper from nitrogen adsorption isotherms.

3.4. Catalytic Activity

The catalytic ceramic papers developed were catalytically evaluated in an equipment consisting of an electric furnace connected to a Novus 1100 temperature controller and programmer, which uses a K-type thermocouple placed at the level of the catalytic bed under study. Inside the furnace, three 16-mm-diameter stacked ceramic paper discs are placed in a quartz tubular reactor. The discs are previously impregnated with a 600 ppm soot suspension, which was obtained directly from the combustion of Repsol YPF-Argentina commercial diesel. The tests were performed in a flow composed of 18% O_2 , 0.1% NO diluted in He (total flow $20 \text{ mL}\cdot\text{min}^{-1}$), heating from room temperature to 600 °C with a ramp of $5^\circ\cdot\text{min}^{-1}$. The GHSV space velocity rate was $12,000 \text{ h}^{-1}$. These conditions were selected because they better represented real conditions and were more comparable to those commonly used by most reports in the literature. The effluent gases were analyzed in a Shimadzu GC-2014 gas chromatograph equipped with a TCD detector.

In all cases, the carbon balance was closed by taking into account the weight of the loaded soot and the area under the curve in TPO experiments, and was always better than 95%.

4. Conclusions

In the present work, the obtaining of ceramic papers and their application as catalytic supports was studied, starting from preparations based on the use of ceramic fibers and ulexite (natural borate) as binder, and incorporating different catalytic systems. Manipulable and mechanically resistant structures were obtained, capable of supporting catalytic particles on the fibrous matrix.

By means of potentiometric titrations and retention values, it was concluded that the dual method adapted to the preparation of this type of structures, which included the addition of the determined amounts of the selected polyelectrolytes (APAM and PVAm), was adequate.

As for the preparation, using 3.2 g of ulexite, and calcining at 650 °C, an optimum was found for which the binder was effective in binding the ceramic fibers, obtaining a tensile index of $0.67 \text{ (N}\cdot\text{m}\cdot\text{g}^{-1})$ and an elasticity of 27.43 (MPa) . The papers thus obtained were manipulable and adaptable to different geometries.

When studying the catalytic activity with both systems incorporated, Co,Ce or Co,Ba,K, good results were achieved, being necessary to obtain a good catalytic behavior the loading of 12% w/w of total active phase with respect to the mass of paper. Lower amounts of active phases (5% w/w) did not favor soot conversion. The best activity was obtained with the Co,Ba,K system ($T_M = 410$ °C) because it is homogeneously distributed both on the fiber and on the binder particles, thus covering the entire exposed surface of the support.

This temperature is in the range of the exhaust gas temperature at the outlet of diesel engines, indicating an avenue for further research. Thus, this system could be considered for a technological application, with a view to its use in processes where the removal of harmful carbonaceous particles is necessary, as in the case of passive regeneration of a diesel catalytic soot filter.

Supplementary Materials: The following supporting information can be downloaded at: <https://www.mdpi.com/article/10.3390/catal12101153/s1>, Figure S1: Identification of the deposits found for the sample Co,Ba,K(12)U-I by spot EDX analysis and Figure S2: Stages of polyelectrolyte titration by charge-flow potential measurements: (a) extracted samples (samples 1–5), (b) centrifugation and (c) potentiometric titration.

Author Contributions: S.A.L. carried out the experiments and the editing of a draft document. E.E.M. contributed to discussions and the interpretation of results and editing of the final version. V.G.M., project director, contributed to discussions and the interpretation of results and editing of the final version. All authors have read and agreed to the published version of the manuscript.

Funding: The authors thank the financial support received from Agencia Nacional de Promoción Científica y Tecnológica (ANPCyT, grant PICT 2019-00976), Consejo Nacional de Investigaciones Científicas y Técnicas (CONICET) and Universidad Nacional del Litoral (UNL, CAI+D2020).

Data Availability Statement: All data and materials support the published claims and comply with field standards.

Acknowledgments: The authors would like to thank the Institute of cellulose Technology (ITC, FIQ, UNL), for the infrastructural facilities for the preparation of ceramic papers.

Conflicts of Interest: The authors declare no conflict of interest.

References

1. Padhi, A.; Bansal, M.; Habib, G.; Samiksha, S.; Raman, R.S. Physical, chemical and optical properties of PM2.5 and gaseous emissions from cooking with biomass fuel in the Indo-Gangetic Plain. *Sci. Total Environ.* **2022**, *841*, 156730. [[CrossRef](#)] [[PubMed](#)]
2. Hama, S.; Ouchen, I.; Wyche, K.P.; Cordell, R.L.; Monks, P.S. Carbonaceous aerosols in five European cities: Insights into primary emissions and secondary particle formation. *Atmos. Res.* **2022**, *274*, 106180. [[CrossRef](#)]
3. Lee, S.; Lim, S.; Lee, H.; Park, S. Probing the oxidation reactivity of ultra-low-sulfur diesel soot with controlled particle size and organic mass fraction. *J. Anal. Appl. Pyrolysis* **2019**, *140*, 264–273. [[CrossRef](#)]
4. Pérez, V.R.; Bueno-López, A. Catalytic regeneration of diesel particulate filters: Comparison of Pt and CePr active phases. *Chem. Eng. J.* **2015**, *279*, 79–85. [[CrossRef](#)]
5. Millo, F.; Andreatta, M.; Ra, M.; Mercuri, D.; Pozzi, C. Impact on vehicle fuel economy of the soot loading on diesel particulate filters made of different substrate materials. *Energy* **2015**, *86*, 19–30. [[CrossRef](#)]
6. Godoy, M.L.; Banús, E.D.; Miró, E.E.; Milt, V.G. Single and double bed stacked wire mesh cartridges for the catalytic treatment of diesel exhaust. *J. Environ. Chem. Eng.* **2019**, *7*, 103290. [[CrossRef](#)]
7. Sacco, N.A.; Banús, E.D.; Milt, V.G.; Miró, E.E.; Bortolozzi, J.P. Catalytic Paper Filters for Diesel Soot Abatement: Studies at Laboratory and Bench Scales. *Emiss. Control Sci. Technol.* **2020**, *6*, 450–461. [[CrossRef](#)]
8. Leonardi, S.A.; Zanuttini, M.A.; Miró, E.E.; Milt, V.G. Catalytic paper made from ceramic fibres and natural ulexite. Application to diesel particulate removal. *Chem. Eng. J.* **2017**, *317*, 394–403. [[CrossRef](#)]
9. Leonardi, S.A.; Tuler, F.E.; Gaigneaux, E.; Debecker, D.P.; Miró, E.E.; Milt, V.G. Novel ceramic paper structures for diesel exhaust purification. *Environ. Sci. Pollut. Res.* **2018**, *25*, 35276–35286. [[CrossRef](#)]
10. Schnell, C.N.; Tarrés, Q.; Galván, M.V.; Mocchiutti, P.; Delgado-Aguilar, M.; Zanuttini, M.A.; Mutjé, P. Polyelectrolyte complexes for assisting the application of lignocellulosic micro/nanofibers in papermaking. *Cellulose* **2018**, *25*, 6083–6092. [[CrossRef](#)]
11. Raunio, J.; Asikainen, T.; Wilo, M.; Kallio, E.; Csóka, L. Affecting the bonding between PLA fibrils and kraft pulp for improving paper dry-strength. *Nord. Pulp Pap. Res. J.* **2020**, *35*, 185–194. [[CrossRef](#)]
12. Salmi, J.; Österberg, M.; Stenius, P.; Laine, J. Surface forces between cellulose surfaces in cationic polyelectrolyte solutions: The effect of polymer molecular weight and charge density. *Nord. Pulp Pap. Res. J.* **2007**, *22*, 249–257. [[CrossRef](#)]
13. Leonardi, S.A.; Miró, E.E.; Milt, V.G. Activity of Catalytic Ceramic Papers to Remove Soot Particles—A Study of Different Types of Soot. *Catalysts* **2022**, *12*, 855. [[CrossRef](#)]
14. Cecchini, J.P.; Serra, R.M.; Ulla, M.A.; Zanuttini, M.A.; Milt, V.G. Enhancing mechanical properties of ceramic papers loaded with zeolites using borates compounds as binders. *Bioresources* **2013**, *8*, 313–326. [[CrossRef](#)]
15. Cecchini, J.P.; Banús, E.D.; Leonardi, S.A.; Zanuttini, M.A.; Ulla, M.A.; Milt, V.G. Flexible-Structured Systems Made of Ceramic Fibers Containing Pt-NaY Zeolite Used as CO Oxidation Catalysts. *J. Mater. Sci.* **2014**, *50*, 755–768. [[CrossRef](#)]
16. Milt, V.G.; Querini, C.A.; Miró, E.E.; Ulla, M.A. Abatement of Diesel Exhaust Pollutants: NO_x Adsorption on Co, Ba, K/CeO₂. *Catalysts. J. Catal.* **2003**, *220*, 424–432. [[CrossRef](#)]
17. Sui, L.; Yu, L. Diesel soot oxidation catalyzed by Co-Ba-K catalysts: Evaluation of the performance of the catalysts. *Chem. Eng. J.* **2008**, *142*, 327–330. [[CrossRef](#)]
18. Banús, E.D.; Milt, V.G.; Miró, E.E.; Ulla, M.A. Co,Ba,K/ZrO₂ coated onto metallic foam (AISI 314) as a structured catalyst for soot combustion: Coating preparation and characterization. *Appl. Catal. A Gen.* **2010**, *379*, 95–104. [[CrossRef](#)]

19. Banús, E.D.; Milt, V.G.; Miró, E.E.; Ulla, M.A. Catalytic coating synthesized onto cordierite monolith walls. Its application to diesel soot combustion. *Appl. Catal. B Environ.* **2013**, *132–133*, 479–486. [[CrossRef](#)]
20. Xing, L.; Yang, Y.; Ren, W.; Zhao, D.; Tian, Y.; Ding, T.; Zhang, J.; Zheng, L.; Lia, X. Highly efficient catalytic soot combustion performance of hierarchically meso-macroporous $\text{Co}_3\text{O}_4/\text{CeO}_2$ nanosheet monolithic catalysts. *Catal. Today* **2020**, *351*, 83–93. [[CrossRef](#)]
21. Zheng, C.; Bao, S.; Mao, D.; Xu, Z.; Zheng, S. Insight into phase structure-dependent soot oxidation activity of K/MnO_2 catalyst. *J. Environ. Sci.* **2022**, *126*, 668–682. [[CrossRef](#)]
22. Xu, H.; Zeng, L.; Cui, L.; Guo, W.; Gong, C.; Xue, G. *In-situ* generation of platinum nanoparticles on LaCoO_3 matrix for soot oxidation. *J. Rare Earths* **2022**, *40*, 888–896. [[CrossRef](#)]
23. Soares, S.; Camino, G.; Levinchik, S. Comparative study of the thermal decomposition of pure cellulose and pulp paper. *Polym. Degrad. Stab.* **1995**, *49*, 275–283. [[CrossRef](#)]
24. Bhardwaj, N.K.; Duong, T.D.; Nguyen, K.L. Pulp charge determination by different methods: Effect of beating/refining. *Colloids Surf. A Physicochem. Eng. Asp.* **2004**, *236*, 39–44. [[CrossRef](#)]